

Exploration of Pipecolate Sulfonamides as Binders of the FK506-Binding Proteins 51 and 52

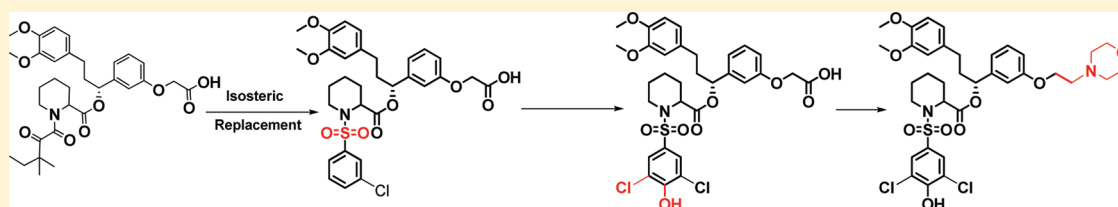
Ranganath Gopalakrishnan,[†] Christian Kozany,[†] Yansong Wang,[†] Sabine Schneider,[§] Bastiaan Hoogeland,[†] Andreas Bracher,[‡] and Felix Hausch^{*,†}

[†]Max Planck Institute of Psychiatry, Kraepelinstrasse 2, 80804 Munich, Germany

[‡]Max Planck Institute of Biochemistry, Am Klopferspitz 18, 82152 Martinsried, Germany

[§]Department Chemie, Technical University Munich, Lichtenbergstrasse 4, 85747 Garching, Germany

S Supporting Information



ABSTRACT: FK506-binding proteins (FKBP) 51 and 52 are cochaperones that modulate the signal transduction of steroid hormone receptors. Single nucleotide polymorphisms in the gene encoding FKBP51 have been associated with a variety of psychiatric disorders. Rapamycin and FK506 are two macrocyclic natural products, which tightly bind to most FKBP family members, including FKBP51 and FKBP52. A bioisosteric replacement of the α -ketoamide moiety of rapamycin and FK506 with a sulfonamide was envisaged with the retention of the conserved hydrogen bonds. A focused solid support-based synthesis protocol was developed, which led to ligands with submicromolar affinity for FKBP51 and FKBP52. The molecular binding mode for one sulfonamide analogue was confirmed by X-ray crystallography.

INTRODUCTION

Members of the FKBP (FK506-binding protein) family display peptidyl prolyl isomerase (PPIase) activity and bind to the immunosuppressive natural products FK506 and rapamycin. The prototypical FKBP12 is the most widely studied member of this family. In complex with FKBP12, FK506 and rapamycin also interact with and inhibit calcineurin (CaN) and mTOR, respectively, thereby mediating their immunosuppressive action. Prior studies led to analogues devoid of immunosuppressive activity,^{1–3} as exemplified by compound **2** (Figure 1).⁴ The high molecular weight, multidomain FKBP51 and FKBP52 act as cochaperones for the heat shock protein 90 (Hsp90) and modulate the signal transduction of the glucocorticoid receptor in a mutually antagonistic direction.^{5–7}

Human genetic studies have shown intronic single nucleotide polymorphisms in the gene encoding FKBP51 to be associated with FKBP51 expression and with various stress-related psychiatric disorders.⁸ Recent characterization of FKBP51 knockout mice has further validated these findings,^{9–12} suggesting that inhibition of FKBP51 might be of therapeutic benefit for psychiatric disorders.³² To further dissect the role of larger FKBP51 and to better understand the underlying biology, selective inhibitors targeting FKBP51 are required. Neither FK506 nor rapamycin can be used as tools as they have nearly equipotent affinities for all FKBP51.

Extensive medicinal chemistry campaigns on analogues of FK506 and rapamycin have shown that the two conserved

hydrogen bonds shown in Figure 1 are required for binding to FKBP51. The electrophilicity of the α -ketoamide moiety present in most of the nonimmunosuppressive FK506 analogues is an undesired reactive liability that could result in metabolic instability or potential toxicity. For FKBP12, it has been shown that the α -ketoamide can be bioisosterically replaced by a sulfonamide moiety to yield compounds that retain binding to FKBP12.^{2,13–15}

However, these compounds have not been tested for their binding profile with the larger FKBP51. Until very recently, compound **2** has been the only synthetic ligand tested for its binding affinity for FKBP51. In the quest for finding improved inhibitors of FKBP51 or FKBP52, we envisaged a solid-phase synthesis methodology for the synthesis of pipecolate sulfonamide compounds to gain insight into the structure–activity relationship (SAR) of this series for the larger FKBP isoforms.

RESULTS AND DISCUSSION

Chemistry. Strategy. A three-dimensional alignment of the FK506-binding domains of FKBP51 (3O5E),¹⁶ FKBP52 (to be published), and FKBP12 (2PPN)¹⁷ revealed the largest structural divergences close to the binding pocket at the 80s loop (Ser¹¹⁸-Ile¹²² of FKBP51/52). The 80s loop of FKBP51 contains Leu¹¹⁹, which is replaced by Pro¹¹⁹ in FKBP52 possibly

Received: December 28, 2011

Published: March 29, 2012

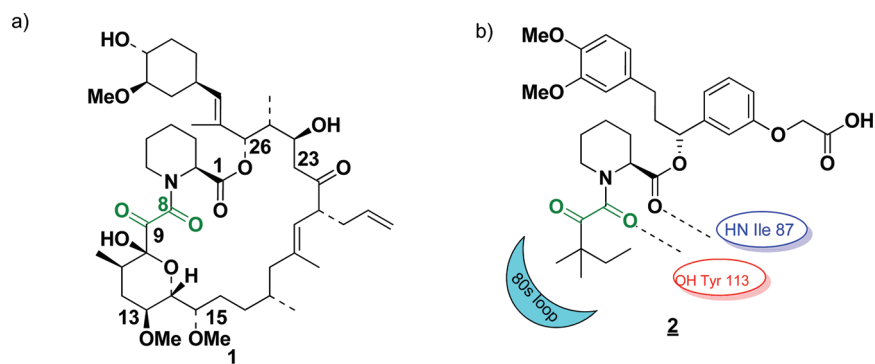
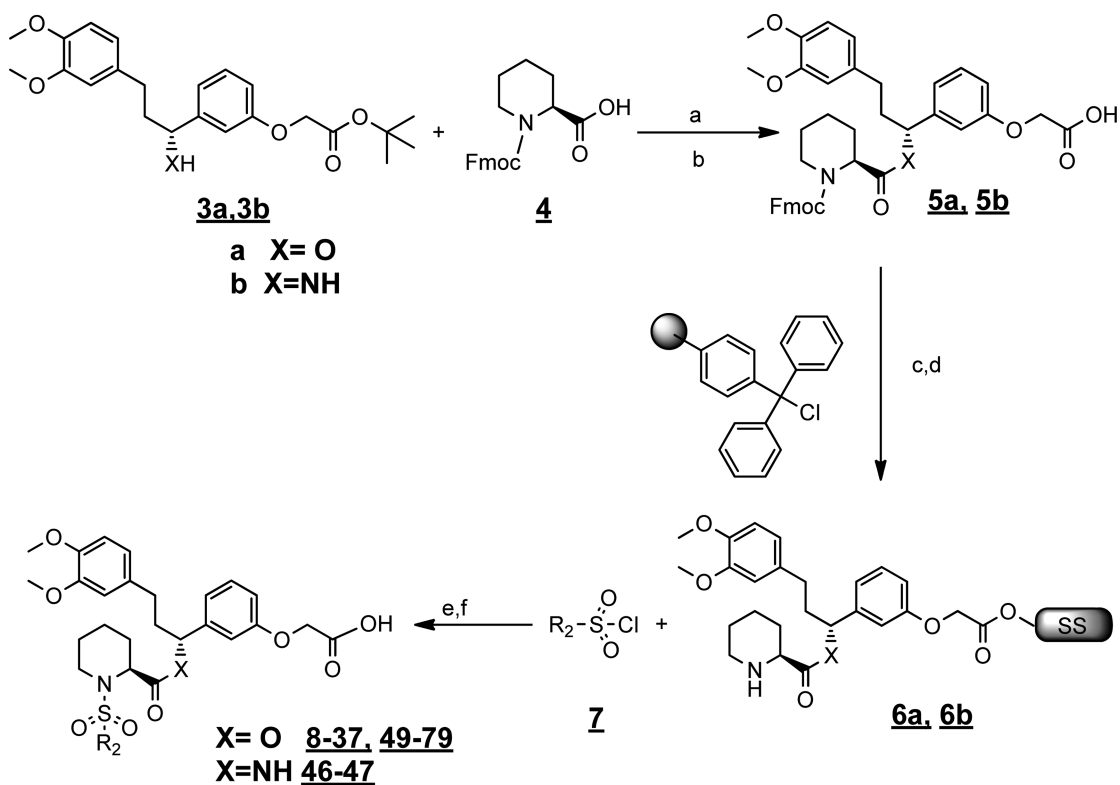


Figure 1. Natural and synthetic ligands that bind to large FKBP5. (a) Structure of FK506 (**1**). (b) The prototypic synthetic ligand **2**, which is devoid of immunosuppressive activity. Key hydrogen bonds with FKBP51 are indicated by dotted lines; the position of the 80s loop interacting with the *tert*-pentyl moiety is indicated in cyan.

Scheme 1. Synthesis of the Pipecolate Framework^a



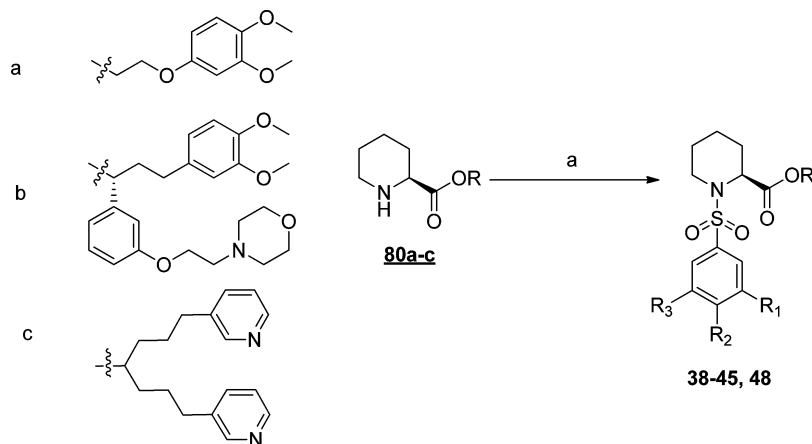
^aReagents and conditions: (a) DCC, DMAP, 0 °C to rt, 20 h (for **3a**); HATU, DIPEA, rt, 2 h (for **3b**). (b) 20% TFA in CH₂Cl₂, rt, 6 h. (c) DIPEA, rt, 4–16 h. (d) 20% 4-methyl-piperidine, CH₂Cl₂, rt, 1 h. (e) DIPEA, CH₂Cl₂, rt, 16 h. (f) 1% TFA in CH₂Cl₂, rt, 1 h.

contributing for the structural difference in this region. Importantly, the residue at position 119 was shown to be a major functional determinant for the effect on steroid hormone receptor.¹⁸ Hence, an optimization of interactions with this part of the protein has a higher probability of achieving selectivity and functional relevance within the FKBP family. The X-ray structures of FK506 with the FK1 domain of FKBP51 (3OSR) and FKBP52 (unpublished) confirmed that the pyranose group in FK506 (**1**) contacts the 80s loop. Sulfonamide substituents as replacements of the pyranose group have been shown to have contact with the 80s loop in FKBP12.^{2,13,14,19} Compound **2**, until very recently the only known synthetic FKBP51 ligand, was chosen as a starting point for the synthesis of sulfonamide analogues. For a rapid derivatization of compounds targeting

the 80s loop, we envisaged a solid-phase strategy for synthesis of a focused sulfonamide library.

Solid-Phase Synthesis of a Focused Sulfonamide Library. The precursor **3** was synthesized as described.²⁰ This was further coupled with the pipericolate **4** followed by liberation of the acid to give the building block **5**. The latter was anchored on a 2-chloro trityl resin (Scheme 1).

The immobilized building block was deprotected to give **6** and was further reacted with a library of commercial sulfonyl chlorides **7**. Cleavage from the solid support under mild acidic conditions yielded compounds **8–37**, **49–79**, and **46** and **47**. This solid support protocol was used for the synthesis of a small focused library followed by primary screening as well as for the resynthesis of hits for further characterization. The best sulfonamide analogues of this

Scheme 2. Synthesis of the Various Top Groups Containing Sulfonamide^a

^aReagent and conditions: (a) DIPEA, RSO₂Cl, CH₂Cl₂, rt, 16 h.

series were further attached to a piperolate core where the free acid containing “top” group in 8–37 and 49–79 was truncated (38–39), exchanged by a morpholine (40–45), or replaced by a pyridine-containing “top” group (Scheme 2).

Biology. The binding of the sulfonamide ligands to FKBP12, FKBP51, and FKBP52 were determined using a competitive fluorescence polarization assays.²¹ The sulfonyl chloride building blocks were designed to initially probe a variety of aliphatic and aromatic sulfonyl moieties as well as substituents around the aromatic rings. Out of 36 compounds in the medium-throughput screening, 28 compounds inhibited tracer binding to FKBP12 by more than 15%, while eight compounds displayed inhibition of more than 85% at 5 μM (Supporting Information and Table 1). Seven compounds

α-ketoamides in the context of this scaffold but that efficient binding critically depended on the nature of the sulfonamide substituent, at least for the larger FKBP. In general, the inhibitory activity was much higher for FKBP12 than for the larger FKBP. This could be related to the core structure 6, which was designed and optimized for FKBP12 as well as to the more concave 80s loop of FKBP12.

The most promising compounds 8–12 from the primary screening were selected, resynthesized in larger scale, and characterized in more detail. The binding affinities of all sulfonamide hits were weaker for all tested FKBP as compared to the reference compound 2. This was most pronounced for FKBP12 for which affinities were reduced by at least 10-fold. It was less apparent for FKBP51, which was only affected by a factor of 2 for compound 10. Compounds 9 and 10 turned out to have the highest binding affinity for FKBP51 and -52 and were further evaluated in two series (Table 2).

Exploration of the SAR. The first series of derivatives probed the influence of the substituent at the meta position. The compounds in this series included *m*-CN 13, *m*-NO₂ 14, *m*-NH₂ 15, *m*-(2-methylpyrimidin-4-yl) 16, *m*-(pyrimidin-4-yl) 17, *m*-F 18, and *m*-Br 19 aromatic sulfonamides. All of these compounds had binding affinity between 0.3 and 10 μM for FKBP12. The meta-substituted halogen derivatives had better binding affinity to the larger FKBP, among these 19 being the best. Compound 15 was synthesized by reduction of the nitro group in 14. The *m*-CN 13, *m*-NO₂ 14, and *m*-NH₂ 15 analogues had slightly reduced binding affinities to the FKBP as compared to the *m*-Cl aromatic sulfonamide 9, while compounds 16 and 17 were inactive for the larger FKBP.

We next set out to explore multisubstituted aromatic sulfonamide groups. The dichloro-substituted aromatic sulfonamide 20 had slightly better binding affinity than the mono *meta*-chloro-substituted aromatic sulfonamide 9 (Table 2). In contrast, an additional chloro-substituent in the para-position 21 was found to substantially reduce binding to the FKBP. A similar result was found for the *meta,para*-dimethoxy-substituted sulfonamide 22, but interestingly, compound 23 having an *m*-Cl, *p*-OMe substitution had better binding affinity. This series of compounds indicated the following SAR *m*-di-Cl > *m*-Cl > *m,p*-di-Cl ≫ *p*-Cl ≫ *o*-Cl for the aryl sulfonamide substituents.

To further explore the acceptable nature of the groups at the meta positions, the derivatives *m*-difluoro 24, 3,5-bis(trifluoromethyl)

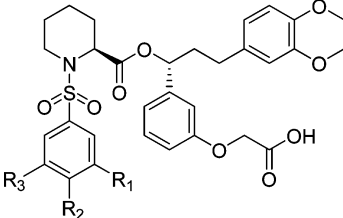
Table 1. Binding Affinities for the Primary Hits towards FKBP Paralogues

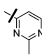
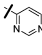
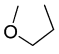
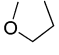
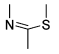
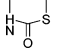
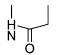
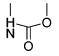
Compd. No.	R	Purity %	FKBP		
			FKBP12	FKBP51FK1	FKBP52FK1
IC ₅₀ (μM) ^a					
2		>99	0.114 ± 0.015	6.3 ± 0.9	9.37 ± 1.9
8		>99	1.8 ± 0.1	62.8 ± 10.7	>100
9		>98	1.2 ± 0.2	30.7 ± 15.7	32.8 ± 14.5
10		>99	1.1 ± 0.1	11.6 ± 1.1	32.5 ± 3.5
11		>96	10.1 ± 1.0	>100	>100
12		>99	4.6 ± 0.15	67.1 ± 12.1	>100

^aBinding affinities to FKBP12, FKBP51 (FK1 domain), and FKBP52 (FK1 domain) were determined by a fluorescence polarization assay.²¹

inhibited the tracer binding to the FK1 domain of FKBP52 by more than 15% at 5 μM, whereas five hits were identified for the FK1 domain of FKBP51. The initial screening assay results indicated that sulfonamides can be surrogates of the

Table 2. Meta-Substituted Analogues Synthesized for SAR Extrapolation



Compd. No.	R1	R2	R3	Purity ^a %	IC ₅₀ (μM) ^b		
					FKBP12	FKBP51FK1	FKBP52FK1
<u>13</u>	CN	H	H	>98	3.8 ± 0.3	28.5 ± 9.6	69.9 ± 65.4
<u>14</u>	NO ₂	H	H	>98	1.9 ± 0.13	47.2 ± 7.1	>100
<u>15</u>	NH ₂	H	H	>99	1.9 ± 0.2	45.4 ± 13.1	>100
<u>16</u>		H	H	>99	8.1 ± 1.2	>100	>100
<u>17</u>		H	H	>99	9.1 ± 0.7	>100	>100
<u>18</u>	F	H	H	>99	1.09 ± 0.07	54.05 ± 7.0	84.5 ± 51.00
<u>19</u>	Br	H	H	>99	0.32 ± 0.03	15.78 ± 1.25	15.69 ± 6.84
<u>20</u>	Cl	H	Cl	>99	0.80 ± 0.08	22.6 ± 8.2	14.3 ± 1.8
<u>21</u>	Cl	Cl	H	>99	6.1 ± 5.7	>100	>100
<u>22</u>	OMe	OMe	H	>96	7.6 ± 1.9	>100	>100
<u>23</u>	Cl	OMe	H	>99	0.60 ± 0.07	29.6 ± 1.9	40.3 ± 5.1
<u>24</u>	F	H	F	>98	1.00 ± 0.06	88.2 ± 11.6	Not measured
<u>25</u>	CF ₃	H	CF ₃	>99	5.1 ± 0.4	>100	>100
<u>26</u>	CF ₃	H	Br	>99	2.4 ± 0.2	>100	>100
<u>27</u>	COOMe	H	COOMe	>98	4.5 ± 0.5	>100	>100
<u>28</u>	Cl	OH	Cl	>99	0.67 ± 0.04	6.2 ± 0.5	20.3 ± 1.9
<u>29</u>	Cl	OMe	Cl	>99	0.23 ± 0.02	16.4 ± 1.7	17.7 ± 1.6
<u>30</u>	Cl	N-Ac	Cl	>98	1.18 ± 0.04	16.1 ± 0.96	20.5 ± 2.7
<u>31</u>	OMe	OMe	COOH	>98	No binding	No binding	No binding
<u>32</u>	NO ₂			>98	1.5 ± 0.14	27.2 ± 3.1	43.9 ± 10.1
<u>33</u>	NH ₂			>98	2.57 ± 0.55	>100	>100
<u>34</u>	H			>98	1.2 ± 0.09	18.4 ± 1.4	26.5 ± 4.9
<u>35</u>	H			>99	0.021 ± 0.02	14.7 ± 1.1	66.5 ± 27.1
<u>36</u>	H			>99	0.66 ± 0.05	>100	>100
<u>37</u>	H			>98	0.75 ± 0.04	>100	>100

^aPurity of the compounds was confirmed by using HPLC. ^bBinding affinities to FKBP12, FKBP51 (FK1 domain), and FKBP52 (FK1 domain) were determined by a fluorescence polarization assay.²¹

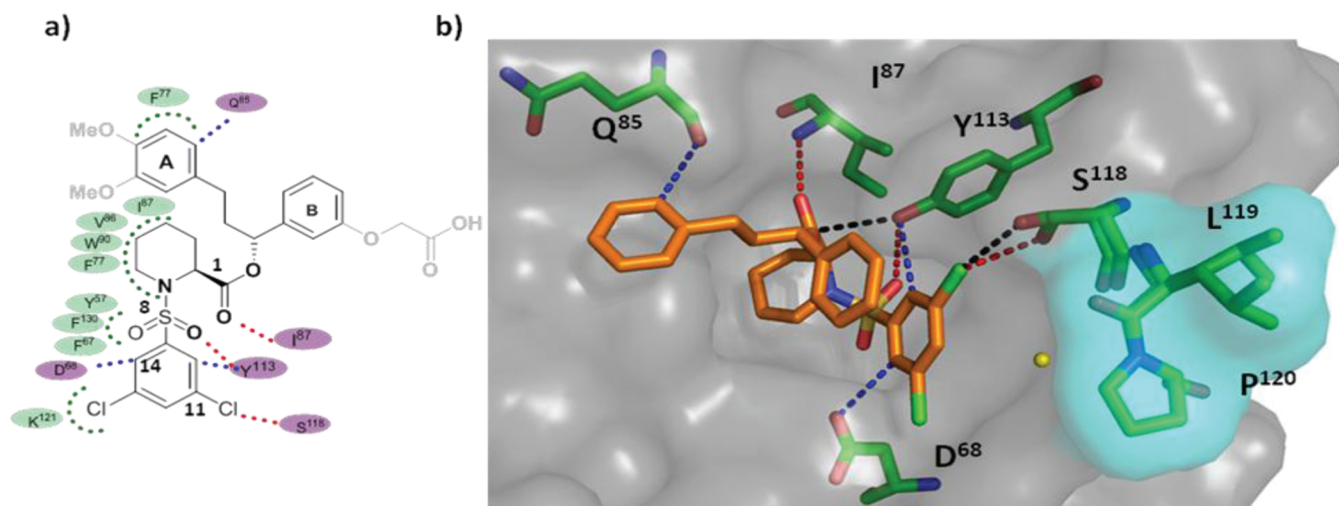


Figure 2. X-ray crystal structure of **20** in complex with the FK1 domain of FKBP51. (a) Chemical structure of **20**. Hydrophobic contacts with FKBP51 are indicated in green, hydrogen bonds are shown as dotted lines in pink, aromatic hydrogen bonds are indicated in blue, and the unresolved groups are in gray. (b) Compound **20** bound to the FK1 domain of FKBP51. The three hydrogen bonds between O¹-**20** and HN-Ile⁸⁷, between O⁸-**20** and HO-Tyr¹¹³, and between Cl¹¹ and O-S¹¹⁸ are shown as dotted red lines. The dipolar interaction between the C¹-carbonyl and HO-Tyr¹¹³ and the halogen bond between Cl¹¹ and O-S¹¹⁸ are shown in black. Aromatic hydrogen bonds between ring A and Gln⁸⁵, C¹⁰-H and OH-Tyr¹¹³, C¹⁴-H and OH-Asp⁶⁸ are shown in blue. Leu¹¹⁹ and Pro¹²⁰ at the top of the 80s loop are colored in cyan, and the conserved water below the 80s loop is shown in yellow.

25, 3-bromo-5-(trifluoromethyl) **26**, and 3,5-bis(carboxy-methyl) **27** were synthesized. Compound **24** had reduced affinity as compared to the monofluoro substituted analogue **18**, while the three other compounds were inactive for FKBP51 or FKBP52. This series led us to conclude that a halogen is a preferred substituent at the meta-position for the larger FKBP5s (Table 2).

The second series of sulfonamide derivatives was designed to probe the substitution pattern at the fused thiazole ring of compound **10**. A substitution by methyl at C-2 resulted in compound **34**, which had equivalent binding to **10**. Conversion to the corresponding benzothiazol-2(3*H*)-one **35** resulted in nanomolar affinity for FKBP12, low micromolar binding for FKBP51, and high micromolar affinity to FKBP52. The reasons for this striking selective preference for FKBP12 are currently unknown. However, the sulfur in the meta-position seems to be extremely important since substitution by a methylene as in **36** or oxygen **37** resulted in a dramatic loss of affinity for all FKBP5s (Table 2).

X-ray Crystal Structure. The X-ray crystal structure of the FK506-binding domain of FKBP51 complexed with ligand **20** was solved to 1.0 Å resolution. In this complex, FKBP51 adopts the same folding topology as found in FKBP51 complexed with **1** and **2**. As compared to the latter structures, Asp⁶⁸ moves into the binding pocket, while Tyr¹¹³ and Ser¹¹⁸ move out. The ligand adopts a similar binding mode as compared to that of **1** or **2** with the common pipercolate ring being nearly superimposable (Figure 2b). The pipercolyl ring of each ligand sits atop the indole of Trp⁹⁰, which forms the floor of the FKBP binding pocket. Similar to FK506, the C¹-carbonyl of the pipercolate forms a hydrogen bond with the backbone amide of Ile⁸⁷. One oxygen of the sulfonamide engages the ϵ -hydrogen of Phe¹³⁰ and the hydroxyl group of Tyr¹¹³. This latter contact is substantially longer (3.37 Å) as compared to the corresponding hydrogen bonds formed between the Tyr¹¹³ and the C⁸-carbonyl groups of α -ketoamides like FK506, **2**, or analogues thereof. The *p*-oxygen of Tyr¹¹³ engages in a rather short dipolar contact with the C¹-carbonyl of **20** (3.06 Å). Similar although less intense dipolar interactions have also been observed in FKBP51 complexes with FK506 and **2**. FKBP51

and **20** engage in a number of aromatic CH \cdots O-acceptor interactions, for example, the oxygen of the sulfonamide and the ϵ -hydrogens of Tyr⁵⁷, Phe⁶⁷, and Phe¹³⁰. These interactions correspond to the contacts formed by the C⁹-keto group of FK506 with the same residues of FKBP51, thereby confirming that the sulfonamide is a bioisosteric mimic of the α -ketoamide moiety. As expected, the dichloro aryl ring sits below the 80s loop and packs on Ile¹²². The tip of the 80s loop (Ser¹¹⁸-Lys¹²¹) diverges from the conformations observed with FK506¹⁶ or synthetic FK506 analogues,²⁰ confirming the conformational flexibility of this region. The two *ortho*-hydrogens of the sulfonylphenyl ring form close contacts (2.95 Å) with the *p*-oxygen of Tyr¹¹³ and with carboxylate of Asp⁶⁸, respectively. One of the aromatic chlorines might form a van der Waals contact with Lys¹²¹, while the other chlorine engages Ser¹¹⁸. For the latter, two conformations seem possible, one compatible with a hydrogen bond to the aromatic chlorine, the other with a linear C-Cl \cdots O geometry consistent with a halogen bond.^{22,23} The dimethoxyphenyl and acetoxyphenyl rings were poorly resolved in the electron density map, indicating strong disorder. In the most populated conformer, the top group is rotated by 120° as compared to compound **2**, most likely stabilized by π - π stacking interactions between the acetoxyphenyl ring B and the dichloro aryl substituent of the sulfonamide. The dimethoxyphenyl ring A stacks on the edge of Phe⁷⁷ and points into a solvent channel. Its *ortho*-hydrogen forms an aromatic hydrogen bond ($d = 2.97$ Å) to the backbone carbonyl of Gln⁸⁵.

SAR Extension. The X-ray cocrystal structure of the sulfonamide **20** revealed a water molecule engaged in a hydrogen bond with the amide of Lys¹²¹ that is situated close to the para-position of the sulfonamide aromatic ring (Figure 2b). Water molecules below Pro¹²⁰ of the 80s loop have been observed in several FKBP51 crystal structures¹⁶ (unpublished observations). We therefore explored whether this conserved water molecule could be engaged by substituents in the para-position of the sulfonamide aromatic ring. Introduction of a *p*-OH substituent in compound **28** did not affect the affinity for FKBP51, while improving the selectivity vs FKBP52 3-fold (Table 2).

Table 3. FKBP Binding Affinity of Sulfonamides with Different Pipercolate Ester Substituents

Compd. No.	R1	R2	R3	Purity %	FKBP12	FKBP51FK1	FKBP52FK1
<u>38</u>	Cl	H	Cl	>98	>100	>100	>100
<u>39</u>	H			>99	0.20 ± 0.10	66.27 ± 37.9	>100
<u>40</u>	Cl	H	Cl	>99	>50 μM ^a	>50 μM ^a	>50 μM ^a
<u>41</u>	H			>98	>50 μM ^a	>50 μM ^a	>50 μM ^a
<u>42</u>	Cl	OH	Cl	>99	0.115 ± 0.014	0.456 ± 0.05	0.71 ± 0.10
<u>43</u>	Cl	OMe	Cl	>99	>50 μM ^a	>50 μM ^a	>50 μM ^a
<u>44</u>	H			>99	0.003 ± 0.0005	2.03 ± 0.09	3.41 ± 0.42
<u>45</u>	Cl	N-Ac	Cl	>99	0.45 ± 0.03	12.3 ± 18.9	8.3 ± 6.8
<u>46</u>	Cl	OH	Cl	>99	>100	>100	>100
<u>47</u>	H			>99	1.4 ± 0.21	>100	>100
<u>48</u>	Cl	OH	Cl	>99	0.87 ± 0.07	9.69 ± 0.76	15.13 ± 0.23

^aLow solubility impaired binding measurements.

A similar trend was observed for the *p*-NHAc-substituted analogue **30** but not in the *p*-OMe-substituted analogue **29**. The trisubstituted analogue **33** had similar affinities as compared to the corresponding monosubstituted derivative **15**, whereas for **32**, the affinities were slightly increased as compared to **14**. The trisubstituted analogue **31** was inactive, similar to the disubstituted analogue **22**.

Modification of the Pipercolate Ester Substituents (Top Group). The charged carboxylic acid attached to ring B in the above series is likely to reduce the cell permeability of these compounds. To remove this undesired property, the free acid moiety was replaced by various groups as shown in Scheme 2 to yield compounds **38–48**. Simplified substituents at C-1 as in compounds **38** and **39** resulted in complete loss of activity for the large FKBP. The next series of compounds included the substitution of the free acid moiety with a morpholine group. Surprisingly, in the morpholine series, phenyl sulfonamides substituted with *meta*-dichloro **40**, with *meta*-dichloro, *p*-OMe **41**, and the benzothiazole analogue **42** were inactive for all FKBP including FKBP12 (Table 3). This could be attributed in part to a detection limit imposed by the lower solubility of these compounds. In striking contrast, the *meta*-dichloro, *para*-hydroxy-substituted analogue **42** displayed submicromolar affinities for all tested FKBP. This potency and the almost equal affinity for the large FKBP versus FKBP12 is remarkable, especially when compared to the very close analogues **22** (carboxyl group instead of morpholine), **40**, **43**

(*para*-hydrogen or *para*-methoxy instead of *para*-hydroxy) and **45** (*para*-NH-acetyl). A similar unexpected activity was observed for the morpholine-containing benzothiazol-2(3*H*)-one analogue **44**, which was much more active than thiazole-containing analogue **41** or the carboxyl derivative **35**. The affinity of **44** for FKBP12 rivaled those of the natural product FK506 (Table 2). The molecular underpinnings for the extraordinary activities of **42** and **44** remain to be established. The physiological consequences of inhibition of FKBP12 are still matter of debate. However, a phase I clinical trial with FK1706, a high-affinity, pan-selective FKBP ligand, did not lead to any obvious adverse side effects, indicating that blockade of FKBP would not be grossly toxic.³¹

Last but not least, we replaced the pipercolate C¹ ester by an amide (**46** and **47**), which completely abolished the binding to larger FKBP. Compound **47** retained substantial binding to FKBP12 in line with the preference of this substituent for FKBP12 observed with **44**. The loss of binding affinity of **46** and **47** can be attributed to the additional hydrogen bond donor that would point in the direction of the aromatic ring when bound in a homologous binding mode as **20**. Finally, in **48**, the top group was replaced by a symmetric top group as present in Biricodar,³ which resulted in equivalent affinity as **28**.

CONCLUSION

Using a bioisosteric replacement strategy, we converted the α -ketoamide motif derived from FK506 and rapamycin into a

sulfonamide motif with conservation of the hydrogen bond pattern as confirmed by the cocrystal structure of **20**. By using a solid-phase synthesis protocol, we were able to generate, screen, and optimize a focused library of these compounds. This led to the identification of aromatic sulfonamides with soft substituents in the meta-position as preferred binders of the larger FKBP. In combination with the morpholine-modified top group, this resulted in a 15–20-fold enhancement in affinity for FKBP51 or FKBP52 as compared to the starting compound **2**. The most advanced compound **42** is the best synthetic ligand known for the large FKBP. Compound **44** has exceptionally high affinity for FKBP12, rivaling those of the natural products FK506 and rapamycin.

EXPERIMENTAL SECTION

Chemistry. All solvents were purchased from Roth, reagents were bought from Aldrich-Fluka, and the sulfonyl chlorides were obtained from Maybridge, Sigma Aldrich, ABCR, or AKos, unless otherwise stated. Chromatographic separations were performed either by manual flash chromatography or by automated flash chromatography using an Interchim-Puriflash 430 with a UV detector. Extracts were dried over MgSO_4 , and the solvents were removed under reduced pressure. Merck F-254 commercial plates were used for analytical TLC to follow the course of reaction and visualized by UV light at either 254 or 365 nm. Silica gel 60 (Merck 70–230 mesh) was used for column chromatography. NMR spectra of all compounds were obtained from the Department of Chemistry and Pharmacy, LMU, on a Bruker AC 300, a Bruker XL 400, or a Bruker AMX 600 at room temperature in deuterio- CDCl_3 with tetramethylsilane (TMS) as an internal standard, unless otherwise stated. Mass spectra (m/z) were recorded on a Thermo Finnigan LCQ DECA XP Plus mass spectrometer at the Max Planck Institute of Psychiatry, while the high-resolution mass spectrometry was carried out at the MPI for Biochemistry (Microchemistry Core Facility) on a Varian Mat711 mass spectrometer. The purity of the compounds was verified by reversed phase HPLC. All of the final compounds synthesized and tested have a purity of more than 95%.

HPLC analysis was carried out using a Jupiter 4 μm Proteo column (250 mm \times 4.6 mm, 5 μm particle size); wavelength: 224 nm, 280 nm; flow rate: 1 mL/min; buffer A: 0.1% TFA in 5% MeCN/water; buffer B: 0.1% TFA in 95% MeCN/water; gradient A: after 1 min of elution with 100% buffer A, linear gradient of 0–100% buffer B for 30 min.

Method LCMS: YMC Pro C-8 (100 mm \times 4.6 mm, 3 μm particle size) column; wavelength: 224 nm, 280 nm; flow rate: 1 mL/min; buffer A: 0.1% HCOOH in 5% MeCN/water; buffer B: 0.1% HCOOH in 95% MeCN/water; gradient B: 1 min 100% buffer A, then linear gradient of 0–100% buffer B for 11 min.

The final compounds were purified using a preparative HPLC Jupiter 10 μm Proteo (250 mm \times 21.7 mm, 10 μm particle size) column. Compounds were dissolved in 40% buffer B, and the purification was carried out with an injection loop volume of 2 mL. Wavelength: 224 nm; flow rate: 25 mL/min; buffer A: 0.1% TFA in 5% MeOH/water; buffer B: 0.1% TFA in 95% MeOH/water; gradient C: 40% B, then a linear gradient of 60–70% B for 15 min.

Coupling of Free Acid **5a to the Trityl Resin.** 2-Chloro trityl resin (6.1 g, 7.9 mmol, Novabiochem) was swollen in DCM for 1 h and added to a mixture of 2-(3-((1R)-1-(1-((9H-fluoren-9-yl)methoxy)carbonyl)piperidine-2-carboxyloxy)-3-(3,4-dimethoxyphenyl)propyl)phenoxy)acetic acid **5a** (2.7 g, 3.97 mmol) and *i*-Pr₂EtN (2 g, 15.89 mmol) in 20 mL of dry DCM. The reaction was monitored by removing aliquots of the reactant mixture (10 μL) over a period of 1–24 h, which were filtered and dried. The analytes were then redissolved in buffer A subjected to HPLC analysis and checked for the disappearance of compound **5a**. The slurry was agitated for 16 h and then filtered. The resin was washed with DCM (3 \times 50 mL), DCM:MeOH:*i*-Pr₂EtN 17:2:1 (3 \times 50 mL), DCM (3 \times 20 mL), DMF (3 \times 25 mL), MeOH (3 \times 50 mL), CHCl_3 (3 \times 50 mL), and diethyl ether (3 \times 50 mL). The resin was dried under high vacuum overnight

to yield a free-flowing resin immobilized with compound **5a**. The loading of the free acid was calculated using Fmoc deprotection and measurement of the Fmoc absorbance.

Coupling of Free Acid **5b to the Trityl Resin.** A loading reaction was carried out as described previously.

Final Library Synthetic Route. Fmoc-protected immobilized pipercolate **5a** was preweighed (approximately 50 mg, 0.019 mmol) and transferred to each of 36 wells of a 96-well parallel synthesis reactor platform obtained from FlexChem peptide synthesis system. The resin was swollen for 1 h in 1 mL of DCM followed by addition of 2 mL of 20% 4-methyl piperidine in DCM, and the reactor was stirred for 1 h for the Fmoc deprotection to give **6a**. The wells were washed with DCM (1 \times 3 mL) by vacuum-assisted filtration. The resins were dried, and the sulfonyl chlorides (0.095 mmol) obtained commercially from Maybridge were weighed (15–40 mg) and added to the wells as a solution in DIPEA (30 mg, 0.237 mmol) in 0.25 mL of DCM for the first coupling and 15 mg (0.119 mmol) in 0.25 mL of DCM for the second coupling with 0.057 mmol (5–12 mg) sulfonyl chloride. The reaction time was 4 h for first coupling and 20 h for the second coupling. The wells were subsequently washed with DCM and ethanol to completely remove excess of unreacted sulfonyl chlorides. The compounds were finally cleaved in presence of 1 mL of 1% TFA solution in DCM for 20 min. Each of the solutions were collected by vacuum filtration and dried by air blowing to give approximately 12 mg of the crude products. The purity of the above crude products was analyzed by HPLC using gradient A, and 36 of these compounds were further purified by preparative HPLC using the gradient B. The remaining compound **50** was purified using ion exchange column chromatography to get rid of the traces of unreacted educt. The purified compounds were characterized using mass spectroscopy and dried under high vacuum to yield approximately 1–3 mg of the final desired sulfonamides.

Medium Scale Synthesis. Deprotection of Fmoc Resin **6a.** The coupled resin **5a** was weighed (210 mg, 0.08 mmol) and added to syringes and swollen in DCM (4 mL) for 1 h, and the Fmoc protecting group was removed using 20% 4-methyl piperidine/DCM (4 mL) for 1 h. After filtration, the resin was washed with DCM (3 \times 5 mL) and used for the next coupling step.

Synthesis of Sulfonamides. To the above resin, *i*-Pr₂EtN (40 mg, 0.317 mmol) in dry DCM (3 mL) was added and stirred for 20 min. To this solution, the sulfonyl chloride (0.237 mmol) in 500 μL of DCM was added, and the reaction was stirred for 4 h at room temperature. After the first coupling step, the resins were filtered, washed with DCM (3 \times 10 mL), and then subjected to second coupling with *i*-Pr₂EtN (30 mg, 0.237 mmol), sulfonyl chloride (0.158 mmol) in DCM (3 mL), and stirred for 16 h at room temperature. The resins were washed with DCM (3 \times 5 mL) and dried to give the derivatized resins. These were reswollen in DCM reacted with 1% TFA/DCM (3 mL) for 1 h and then washed with 1% TFA/DCM (3 \times 3 mL) and further washed with DCM (3 \times 5 mL). The combined filtrates were concentrated in vacuo to yield the compounds **8–37** (crude weight \sim 50 mg). The crude compounds were further purified by preparative HPLC using gradient C. The purified peaks were further dried by lyophilization.

Synthesis of 2-(3-((R)-1-((S)-1-(3,5-Dichlorophenylsulfonyl)piperidine-2-carboxyloxy)-3-(3,4-dimethoxyphenyl)propyl)phenoxy)acetic Acid (20**).** TLC (hexane:EtOAc:TFA 5.5:4.5:0.2): R_f = 0.58, yield = 22.6 mg (44%). HPLC (gradient A) retention time = 26.8–27.3 min. ¹H NMR (600 MHz, CDCl_3) δ = 1.03–1.10 (m, 1H), 1.40–1.47 (m, 1H), 1.60–1.63 (m, 2H), 1.71–1.77 (m, 1H), 1.99–2.06 (m, 1H), 2.16–2.23 (m, 2H), 2.49–2.59 (m, 2H), 3.20 (dt, 1H, J = 2.4 Hz, 12.6 Hz), 3.71 (td, 1H, J = 1.2, 12.6 Hz), 3.85 (s, 3H), 3.86 (s, 3H), 4.66 (s, 2H), 4.78 (d, 1H, J = 4.8 Hz), 5.63 (dd, 1H, J = 6 Hz), 6.66–6.68 (m, 2H), 6.79 (d, 1H, J = 7.8 Hz), 6.83–6.84 (m, 1H), 6.85 (t, 1H, J = 2.4 Hz), 6.90 (d, 1H, J = 7.8 Hz), 7.26 (dd, 1H, J = 7.8 Hz), 7.49 (t, 1H, J = 1.8 Hz), 7.66 (d, 1H, J = 1.8 Hz). ¹³C NMR (150 MHz, CDCl_3) δ = 19.74, 24.61, 27.74, 31.28, 37.84, 42.89, 55.32, 55.92, 64.78, 76.65, 111.33, 111.75, 112.95, 114.17, 120.00, 120.17, 125.45, 129.87, 132.42, 133.21, 135.73, 141.63, 142.89, 147.40, 148.86, 157.53, 169.57, 172.53. MS (ESI) m/z : found R_t 14.33 min.

Method LCMS, 688.19, 690.19 [M + Na]⁺. HRMS: 666.1753, 668.1713 [M + H]⁺; calculated, 666.1753 [M + H]⁺.

Synthesis of 2-(3-((R)-1-((S)-1-(3,5-Dichloro-4-hydroxyphenylsulfonyl)piperidine-2-carbonyloxy)-3-(3,4-dimethoxyphenyl)propyl)phenoxy)acetic Acid (28). TLC (hexane:EtOAc:TFA 4.8:5:0.2): $R_f = 0.50$, yield = 12.3 mg (23%). HPLC (gradient A) retention time = 26.8–27.1 min. ¹HNMR (300 MHz, CDCl₃) $\delta = 1.00$ – 1.10 (m, 1H), 1.38– 1.53 (m, 1H), 1.60– 1.68 (m, 2H), 1.74– 1.87 (m, 1H), 2.01– 2.12 (m, 1H), 2.16– 2.26 (m, 2H), 2.53– 2.62 (m, 2H), 3.21 (t, 1H, $J = 12$ Hz), 3.72 (d, 1H, $J = 12$ Hz), 3.87 (s, 6H), 4.65 (s, 2H), 4.77 (d, $J = 2.7$ Hz), 5.63 (t, $J = 6$ Hz), 6.69– 6.71 (m, 2H), 6.80– 6.93 (m, 4H), 7.28 (s, 1H), 7.78 (s, 1H), 7.99 (s, 1H). ¹³C NMR (75 MHz, CDCl₃) $\delta = 19.66$, 24.66, 27.85, 31.34, 37.88, 43.01, 55.4, 55.95, 64.82, 77.21, 111.44, 111.83, 113.02, 114.23, 119.84, 120.21, 122.20, 127.86, 128.97, 129.89, 139.94, 141.75, 145.83, 147.22, 148.89, 153.52, 157.56, 169.51, 172.35. MS (ESI) m/z : found R_t 13.66 min. Method LCMS, 704.68 [M + Na]⁺. HRMS: 682.1962, 684.1949 [M + H]⁺; calculated, 682.1902 [M + H]⁺.

Synthesis of 2-(3-((R)-3-(3,4-Dimethoxyphenyl)-1-((S)-1-(2-oxo-2,3-dihydrobenzo[d]thiazol-6-ylsulfonyl)piperidine-2-carbonyloxy)-propyl)phenoxy)acetic Acid (35). TLC (DCM:MeOH 9.7:0.3): $R_f = 0.37$, yield = 24.20 mg (46.8%). HPLC (gradient A) retention time = 22.74– 22.94 min. ¹HNMR (600 MHz, CDCl₃) $\delta = 1.38$ – 1.45 (m, 1H), 1.59– 1.66 (m, 1H), 1.73– 1.75 (m, 2H), 1.89– 1.99 (m, 2H), 2.09– 2.16 (m, 2H), 2.41– 2.46 (m, 1H), 2.52– 2.57 (m, 1H), 3.23 (t, 1H, $J = 10.2$ Hz), 3.78 (d, 1H, $J = 7.8$ Hz), 3.82 (s, 3H), 3.83 (s, 3H), 4.72– 4.82 (m, 3H), 5.41– 5.43 (m, 1H), 6.18 (d, 1H, $J = 8.4$ Hz), 6.58– 6.65 (m, 3H), 6.76 (d, 1H, $J = 8.4$ Hz), 6.92 (d, 1H, $J = 6.6$ Hz), 7.01 (d, 1H, $J = 8.4$ Hz), 7.09 (d, 1H, $J = 8.4$ Hz), 7.41 (t, 1H, $J = 7.8$ Hz), 7.66 (d, 1H, $J = 1.8$ Hz). ¹³C NMR (150 MHz, CDCl₃) $\delta = 19.52$, 24.83, 28.47, 31.44, 38.63, 42.16, 54.77, 55.85, 55.92, 64.28, 75.54, 111.34, 111.60, 111.69, 113.56, 118.85, 120.12, 121.10, 124.32, 125.93, 130.27, 133.04, 133.23, 138.48, 142.51, 147.43, 148.89, 157.44, 169.46, 172.87, 173.00. MS (ESI) m/z : found R_t 11.08 min. Method LCMS, 693.26 [M + Na]⁺. HRMS: 671.2268 [M + H]⁺; calculated, 671.2255 [M + H]⁺.

General Procedure for the Synthesis of Compounds 40–45.

To **80b** (19 mg, 0.037 mmol), DIPEA (9.2 mg, 0.055 mmol) and the corresponding sulfonyl chloride (0.055 mmol) were added. The reaction was stirred at room temperature overnight and was purified by preparative HPLC using gradient C to yield compounds 40–45.

Synthesis of (S)-((R)-3-(3,4-Dimethoxyphenyl)-1-(3-(2-morpholinoethoxy)phenyl)propyl)-1-(3,5-dichloro-4-hydroxyphenylsulfonyl)piperidine-2-carboxylate (42). TLC (DCM:MeOH 9.7:0.3): $R_f = 0.45$, yield = 15.96 mg (58%). HPLC (gradient A) retention time = 19.28– 19.61 min. ¹HNMR (300 MHz, CDCl₃) $\delta = 1.54$ – 2.06 (m, 6H), 2.14– 2.30 (m, 2H), 2.44– 2.64 (m, 2H), 2.99– 3.27 (m, 3H), 3.51 (s, 2H), 3.74– 3.80 (m, 3H), 3.86 (s, 3H), 3.87 (s, 3H), 4.06 (s, 4H), 4.43 (s, 2H), 4.72 (d, 1H, $J = 4.2$ Hz), 5.53– 5.59 (m, 1H), 6.65– 6.69 (m, 3H), 6.78– 6.85 (m, 2H), 6.92 (d, 1H, $J = 7.8$ Hz), 7.29– 7.33 (m, 1H), 7.49 (s, 2H). ¹³C NMR (75 MHz, CDCl₃) $\delta = 20.15$, 24.94, 28.07, 31.45, 37.87, 42.86, 53.05, 55.25, 55.87, 55.95, 56.81, 62.50, 63.96, 76.25, 111.39, 111.71, 112.71, 114.02, 119.57, 120.15, 121.53, 127.30, 130.22, 132.31, 133.18, 141.75, 147.47, 148.95, 151.71, 157.01, 169.52. MS (ESI) m/z : found R_t 8.76 min. Method LCMS, 737.04, 739.13 [M + H]⁺. HRMS: 737.2532, 739.2506 [M + H]⁺; calculated, 737.2501, 739.2542 [M + H]⁺.

Synthesis of (S)-((R)-3-(3,4-Dimethoxyphenyl)-1-(3-(2-morpholinoethoxy)phenyl)propyl)-1-(2-oxo-2,3-dihydrobenzo[d]thiazol-6-ylsulfonyl)piperidine-2-carboxylate (44). TLC (DCM:MeOH 9.7:0.3): $R_f = 0.39$, yield = 6.4 mg (24.6%). HPLC (gradient A) retention time = 18.92– 19.16 min. ¹HNMR (300 MHz, CDCl₃) $\delta = 1.71$ – 1.81 (m, 2H), 1.84– 2.01 (m, 2H), 2.06– 2.22 (m, 2H), 2.39– 2.62 (m, 2H), 3.01– 3.12 (m, 2H), 3.26– 3.37 (m, 2H), 3.54 (s, 2H), 3.80– 3.91 (m, 12H), 4.06 (s, 4H), 4.26– 4.50 (m, 2H), 4.74 (d, 1H, $J = 4.8$ Hz), 5.36– 5.41 (m, 1H), 6.55– 6.64 (m, 4H), 6.77 (d, 1H, $J = 7.5$ Hz), 6.89 (d, 1H, $J = 6.9$ Hz), 6.99 (d, 1H, $J = 7.5$ Hz), 7.19 (d, 1H, $J = 8.4$ Hz), 7.38 (t, 1H, $J = 7.6$ Hz), 7.62 (d, 1H, $J = 1.8$ Hz). ¹³C NMR (75 MHz, CDCl₃) $\delta = 24.98$, 28.29, 31.43, 38.45, 42.48, 53.47, 54.79, 55.87, 55.94, 57.28, 62.02, 63.93, 75.83, 111.03, 111.37, 111.69, 112.73, 113.79, 119.18, 120.17, 121.54, 124.28, 125.73,

130.46, 133.10, 133.39, 138.88, 142.22, 147.47, 148.93, 156.99, 169.62. MS (ESI) m/z : found R_t 9.47 min. Method LCMS, 726.29 [M + H]⁺. HRMS: 726.3111 [M + H]⁺; calculated, 726.3091 [M + H]⁺.

Deprotection of Fmoc (Resin 6b). The coupled resin **5b** was weighed (190 mg, 0.05 mmol) and added to syringes and swollen in DCM (4 mL) for 1 h, and the Fmoc protecting group was removed using 20% 4-methyl piperidine/DCM (4 mL) for 1 h. After filtration, the resin was washed with DCM (3 × 5 mL) and used for the next coupling step.

Synthesis of Sulfonamides. To the above resin, *i*-Pr₂EtN (25 mg, 0.20 mmol) in dry DCM (3 mL) was added and stirred for 20 min. To this solution, the sulfonyl chloride (0.15 mmol) in 500 μ L of DCM was added, and the reaction was stirred for 4 h at room temperature. After the first coupling step, the resins were filtered, washed with DCM (3 × 10 mL), and then subjected to second coupling with *i*-Pr₂EtN (30 mg, 0.237 mmol) and sulfonyl chloride (0.158 mmol) in DCM (3 mL) and stirred for 16 h at room temperature. The resins were washed with DCM (3 × 5 mL) and dried to give the derivatized resins. These were reswollen in DCM reacted with 1% TFA/DCM (3 mL) for 1 h and then washed with 1% TFA/DCM (3 × 3 mL) and further washed with DCM (3 × 5 mL). The combined filtrates were concentrated in vacuo to yield the compounds **46** and **47**. (crude weight ~ 50 mg). The crude compounds were further purified by preparative HPLC using gradient C. The purified peaks were further dried by lyophilization.

X-ray Crystallography. Crystals and cocrystals of the FKBP51 Fk1 domain construct comprising residues 16–140 and containing mutation A19T were obtained as previously described.¹⁶ Diffraction data were collected at beamline X06DA of the Swiss Light Source (SLS) synchrotron in Villigen, Switzerland. The data were processed with MOSFLM²⁴ and XDS,²⁵ SCALA,²⁶ and TRUNCATE.²⁷ The crystal structure was isomorphous with the apo structure (PDB code 3O5R). The dictionaries for the ligand compounds were generated with the PRODRG server.²⁸ The structures were refined with REFMAC.²⁹ Manual model building was performed with COOT.³⁰ Molecular graphic figures were generated using PyMOL (<http://www.pymol.org>).

■ ASSOCIATED CONTENT

● Supporting Information

Purity and activity data for compounds 47–77 from the high-throughput synthesis and assay. Experimental data of **5a,b**, **8–19**, **21–27**, **29–34**, **36–41**, **43**, and **45–48**. This material is available free of charge via the Internet at <http://pubs.acs.org>.

■ AUTHOR INFORMATION

Corresponding Author

*Tel: +49(89)30622640. Fax: +49(89)30622610. E-mail: hausch@mpipsykl.mpg.de.

Notes

The authors declare no competing financial interest.

■ ACKNOWLEDGMENTS

We thank Dr. Gerd Rührter and the Lead Discovery Center (Dortmund) for providing the precursor for the synthesis of morpholine analogues and compound **46**. We thank Prof. Florian Holsboer and the CIPSM for financial support. We are indebted to Mrs. E. Weyher and Dr. S. Uebel (MPI of Biochemistry) and to Mrs. C. Dubler (Ludwig-Maximilians-Universität Munich) for HRMS and NMR measurements. This research project has been supported by the European Commission under the seventh Framework Program: Research Infrastructures. Grant Agreement Number 226716.

■ ABBREVIATIONS USED

FKBP, FK506-binding protein; Hsp90, heat shock protein 90; SAR, structure–activity relationship

REFERENCES

- (1) Holt, D. A.; Luengo, J. I.; Yamashita, D. S.; Oh, H. J.; Konilian, A. L.; et al. Design, synthesis, and kinetic evaluation of high-affinity FKBP ligands and the X-ray crystal structures of their complexes with FKBP 12. *J. Am. Chem. Soc.* **1993**, *115*, 9925–9938.
- (2) Hudack, R. A. Design, Synthesis, and Biological Activity of Novel Polycyclic Aza-Amide FKBP12 Ligands. *J. Med. Chem.* **2006**, *49*, 1202–1206.
- (3) Gaali, S.; Gopalakrishnan, R.; Wang, Y.; Kozany, C.; Hausch, F. The chemical biology of immunophilin ligands. *Curr. Med. Chem.* **2011**, *18*, 5355–5379.
- (4) Keenan, T.; Yaeger, D. R.; Courage, N. L.; Rollins, C. T.; Pavone, M. E.; et al. Synthesis and activity of bivalent FKBP12 ligands for the regulated dimerization of proteins. *Bioorg. Med. Chem.* **1998**, *6*, 1309–1335.
- (5) Riggs, D. L.; Roberts, P. J.; Chirillo, S. C.; Cheung-Flynn, J.; Prapapanich, V.; et al. The Hsp90-binding peptidylprolyl isomerase FKBP52 potentiates glucocorticoid signaling in vivo. *EMBO J.* **2003**, *22*, 1158–1167.
- (6) Wochnik, G. M.; Ruegg, J.; Abel, G. A.; Schmidt, U.; Holsboer, F.; et al. FK506-binding Proteins 51 and 52 Differentially Regulate Dynein Interaction and Nuclear Translocation of the Glucocorticoid Receptor in Mammalian Cells. *J. Biol. Chem.* **2005**, *280*, 4609–4616.
- (7) Davies, T. H.; Ning, Y.-M.; Sanchez, E. R. Differential control of glucocorticoid receptor hormone-binding function by tetratricopeptide repeat (TPR) proteins and the immunosuppressive ligand FK506. *Biochemistry* **2005**, *44*, 2030–2038.
- (8) Binder, E. B. The role of FKBP5, a co-chaperone of the glucocorticoid receptor in the pathogenesis and therapy of affective and anxiety disorders. *Psychoneuroendocrinology* **2009**, *34*, S186–S195.
- (9) Touma, C.; Gassen, N. C.; Herrmann, L.; Cheung-Flynn, J.; Bull, D. R.; et al. FK506 Binding Protein 5 Shapes Stress Responsiveness: Modulation of Neuroendocrine Reactivity and Coping Behavior. *Biol. Psychiatry* **2011**, *70*, 928–936.
- (10) Hartmann, J.; Wagner, K. V.; Liebl, C.; Scharf, S. H.; Wang, X. D.; et al. The involvement of FK506-binding protein 51 (FKBP5) in the behavioral and neuroendocrine effects of chronic social defeat stress. *Neuropharmacology* **2012**, *62*, 332–339.
- (11) Attwood, B. K.; Bourgoignon, J. M.; Patel, S.; Mucha, M.; Schiavon, E.; et al. Neuropsin cleaves EphB2 in the amygdala to control anxiety. *Nature* **2011**, *473*, 372–375.
- (12) O'Leary, J. C.; Dharia, S.; Blair, L. J.; Brady, S.; Johnson, A. G.; et al. A New Anti-Depressive Strategy for the Elderly: Ablation of FKBP5/FKBP51. *PLoS One* **2011**, *6*, e24840.
- (13) Choi, C.; Li, J. H.; Vaal, M.; Thomas, C.; Limburg, D.; et al. Use of parallel-synthesis combinatorial libraries for rapid identification of potent FKBP12 inhibitors. *Bioorg. Med. Chem. Lett.* **2002**, *12*, 1421–1428.
- (14) Wei, L.; Wu, Y. Q.; Wilkinson, D. E.; Chen, Y.; Soni, R.; et al. Solid-phase synthesis of FKBP12 inhibitors: N-sulfonyl and N-carbamoylprolyl/pipicolyl amides. *Bioorg. Med. Chem. Lett.* **2002**, *12*, 1429–1433.
- (15) Juli, C.; Sippel, M.; Jager, J.; Thiele, A.; Weiwad, M.; et al. Pipecolic Acid Derivatives As Small-Molecule Inhibitors of the Legionella MIP Protein. *J. Med. Chem.* **2011**, *54*, 277–283.
- (16) Bracher, A.; Kozany, C.; Thost, A. K.; Hausch, F. Structural characterization of the PPIase domain of FKBP51, a cochaperone of human Hsp90. *Acta Crystallogr., Sect. D: Biol. Crystallogr.* **2011**, *67*, 549–559.
- (17) Szep, S.; Park, S.; Boder, E. T.; Van Duyne, G. D.; Saven, J. G. Structural coupling between FKBP12 and buried water. *Proteins: Struct., Funct., Bioinf.* **2009**, *74*, 603–611.
- (18) Riggs, D. L.; Cox, M. B.; Tardif, H. L.; Hessling, M.; Buchner, J.; et al. Noncatalytic role of the FKBP52 peptidyl-prolyl isomerase domain in the regulation of steroid hormone signaling. *Mol. Cell. Biol.* **2007**, *27*, 8658–8669.
- (19) Sun, F.; Li, P. Y.; Ding, Y.; Wang, L. W.; Bartlam, M.; et al. Design and structure-based study of new potential FKBP12 inhibitors. *Bioophys. J.* **2003**, *85*, 3194–3201.
- (20) Gopalakrishnan, R.; Kozany, C.; Gaali, S.; Kress, C.; Hoogeland, B.; Bracher, A.; Hausch, F. Evaluation of Synthetic FK506 Analogs as Ligands for the FK506-Binding Proteins 51 and 52. *J. Med. Chem.* **2012**, DOI: 10.1021/jm201746x.
- (21) Kozany, C.; Marz, A.; Kress, C.; Hausch, F. Fluorescent probes to characterise FK506-binding proteins. *ChemBioChem* **2009**, *10*, 1402–1410.
- (22) Bissantz, C.; Kuhn, B.; Stahl, M. A medicinal chemist's guide to molecular interactions. *J. Med. Chem.* **2010**, *53*, 5061–5084.
- (23) Hardegger, L. A.; Kuhn, B.; Spinnler, B.; Anselm, L.; Ecabert, R.; et al. Systematic investigation of halogen bonding in protein-ligand interactions. *Angew. Chem., Int. Ed. Engl.* **2011**, *50*, 314–318.
- (24) Leslie, A. G. W. Recent changes to the MOSFLM package for processing film and image plate data. *Jnt CCP4/ESF-EACMB Newsl Protein Crystallogr.* **1992**, *26*.
- (25) Kabsch, W. Xds. *Acta Crystallogr., Sect. D: Biol. Crystallogr.* **2010**, *66*, 125–132.
- (26) Evans, P. R. SCALA. *Jnt CCP4/ESF-EACMB Newsl. Protein Crystallogr.* **1997**, *33*, 22–24.
- (27) French, S.; Wilson, K. Treatment of Negative Intensity Observations. *Acta Crystallogr., Sect. A* **1978**, *34*, 517–525.
- (28) Schuttelkopf, A. W.; van Aalten, D. M. F. PRODRG: A tool for high-throughput crystallography of protein-ligand complexes. *Acta Crystallogr., Sect. D: Biol. Crystallogr.* **2004**, *60*, 1355–1363.
- (29) Murshudov, G. N.; Skubak, P.; Lebedev, A. A.; Pannu, N. S.; Steiner, R. A.; et al. REFMAC5 for the refinement of macromolecular crystal structures. *Acta Crystallogr., Sect. D: Biol. Crystallogr.* **2011**, *67*, 355–367.
- (30) Emsley, P.; Lohkamp, B.; Scott, W. G.; Cowtan, K. Features and development of Coot. *Acta Crystallogr., Sect. D: Biol. Crystallogr.* **2010**, *66*, 486–501.
- (31) Minematsu, T.; Lee, J.; Zha, J.; Moy, S.; Kowalski, D.; Hori, K.; Ishibashi, K.; Usui, T.; Kamimura, H. Time-dependent inhibitory effects of (1R,9S,12S,13R,14S,17R,18E,21S,23S,24R,25S,27R)-1,14-dihydroxy-12-(E)-2-[(1R,3R,4R)-4-hydroxy-3-methoxy-cyclohexyl]-1-methylvinyl-23,25-dimethoxy-13,19,21,27-tetramethyl-17-(2-oxo-propyl)-11,28-dioxo-4-azatricyclo[22.3.1.0(4,9)]octacos-18-ene-2,3,10,16-tetrone (FK1706), a novel nonimmunosuppressive immunophilin ligand, on CYP3A4/5 activity in humans in vivo and in vitro. *Drug Metab. Dispos.* **2010**, *38* (2), 249–259.
- (32) Schmidt, M. V.; Paez-Pereda, P.; Holsboer, F.; Hausch, F. The prospect of FKBP51 as a drug target. *ChemMedChem* **2012**, DOI: 10.1002/cmdc.201200137.